

# NATIONAL INSTITUTE FOR FUSION SCIENCE

## Constructing Exactly Conservative Scheme in Non-conservative Form

R. Tanaka, T. Nakamura and T. Yabe

(Received - July 16, 1999 )

NIFS-608

Aug. 1999

This report was prepared as a preprint of work performed as a collaboration research of the National Institute for Fusion Science (NIFS) of Japan. This document is intended for information only and for future publication in a journal after some rearrangements of its contents.

Inquiries about copyright and reproduction should be addressed to the Research Information Center, National Institute for Fusion Science, Oroshi-cho, Toki-shi, Gifu-ken 509-02 Japan.

**RESEARCH REPORT**  
NIFS Series

# Constructing exactly conservative scheme in a non- conservative form

**R.Tanaka, T.Nakamura and T.Yabe**

*Department of Energy Sciences,  
Tokyo Institute of Technology,  
4259 Nagatsuta Midori-ku Yokohama 226-8502, Japan*

## Abstract

A non-conservative scheme that guarantees exact mass conservation is proposed. Although it is in a non-conservative form, the mass of each cell is employed as an additional variable that is advanced in a conservative form. Some numerical tests are carried out to demonstrate the mass conservation and the accurate calculation of the speed of a shock wave even without the viscosity term.

**Keywords:** CIP, Computational algorithm, Mass conservation, Semi-Lagrangian.

## 1.Introduction

There have been revolutionary progresses in the numerical solutions of the hyperbolic equations for the last two decades. Among them, the CIP (Cubic-Interpolated Propagation) scheme[1,2,3] is developed by one of the authors almost 15 years ago and has been applied to various multi-phase flows like milk-crown formation[3], laser-induced melting, evaporation[4], and so on. The CIP has many characteristics that is suited for calculation such as capturing surface, even with 1000 times density ratio, and treating incompressible and compressible fluids together. Since it uses primitive Euler representation of equations, it is well suited for multi-phase flow calculations.

In some special cases, however, there exist subjects that require exact conservation of mass, etc. One of the typical example is the black-hole formation and emission of gravity wave[5]. In this case, small fraction of mass is converted into gravity wave and strict mass conservation is essential. Another example is plasma simulation in which Vlasov equation in six-dimensional phase space must be solved and total density of particle must be conserved, otherwise large electric field appears. The CIP method can be constructed to exactly conserve the total mass in Vlasov system of equally spaced grid in phase space[6]. However, the use of non-equally spaced grid or other general grids can save the computational cost and is worthy for investigation.

The CIP method belongs to a class of semi-Lagrangian scheme[7,8], which employs the separate treatment of advection term from other terms and hence enables the advection calculation with large time step free from CFL condition.

Although the semi-Lagrangian scheme has been successfully used in short-term atmospheric problems, the loss of exact conservation makes the scheme inappropriate for long-term problems and oceanic problems. In this sense, the effort to establish exact conservation in semi-Lagrangian form would be a challenging task.

In this paper, we shall propose a non-conservative scheme or a semi-Lagrangian scheme that guarantees exact mass conservation.

## 2.Formulation

Before introducing the scheme, we had better introduce the definition of mass conservation. We discuss at first how to compute conservation law as follows;

$$\frac{\partial f}{\partial t} + \frac{\partial(uf)}{\partial x} = 0. \quad (1)$$

Integrating Eq.(1) from  $x_{i-1/2}$  to  $x_{i+1/2}$  gives an equation

$$\int_{x_{i-1/2}}^{x_{i+1/2}} f^{n+1} dx = \int_{x_{i-1/2}}^{x_{i+1/2}} f^n dx - \Delta t \left( (uf)_{i+1/2}^{n+1/2} - (uf)_{i-1/2}^{n+1/2} \right). \quad (2)$$

If we assume  $f$  being constant  $f_i$  during spatial integration and take the sum of both sides of Eq.(2) over an entire domain, flux defined at cell boundary  $(uf)_{i\pm 1/2}$  cancels each other leading to the conservation of the total mass as follows;

$$\sum_i f_i^{n+1} = \sum_i f_i^n. \quad (3)$$

under an appropriate boundary condition that ensures mass conservation

However, as clear from the procedure leading

to Eq.(3), an accurate conservation condition isn't that shown by Eq.(3), because Eq.(3) is derived under the assumption that  $f$  is spatially uniform between  $x_{i-1/2}$  and  $x_{i+1/2}$ . The more accurate expression for conservation should be given by the integration like the following equation;

$$\int f^{n+1} dx = \int f^n dx. \quad (4)$$

In this paper, we use this definition of mass. Introducing the mass of each cell as

$$\rho_{i+1/2}^n = \int_{x_i}^{x_{i+1}} f^n dx, \quad (5)$$

then Eq.(4) can be put into a form

$$\sum_i \rho_{i+1/2}^{n+1} = \sum_i \rho_{i+1/2}^n. \quad (6)$$

The present scheme employs this  $\rho$  defined by Eq.(5) as an additional variable together with  $f$  in Eq.(1). In the scheme proposed below,  $f$  is advanced in the non-conservative form, but conservation is realized by  $\rho$  which is advanced in a conservative form under the accurate conservation condition of Eq.(4).

For simplicity, we shall start at first with the following advection equation with velocity  $u(\geq 0)$  being constant,

$$\frac{\partial f}{\partial t} + u \frac{\partial f}{\partial x} = 0. \quad (7)$$

Therefore, the time development of  $f$  in Eq.(7) is calculated from the following equation;

$$f(x_i, t + \Delta t) = f(x_i - u\Delta t, t). \quad (8)$$

Here  $f$  is given only at the grid points  $x_1, x_2, \dots, x_i, \dots, x_{\max}$ . We must construct a piecewise interpolation function  $F_i(x)$  on each interval  $[x_{i-1}, x_i]$  to represent  $f(x_i - u\Delta t, t)$ , because if  $u \geq 0$ ,  $f(x_i - u\Delta t, t)$  is located between grids  $[x_{i-1}, x_i]$  in the case of  $CFL \equiv u\Delta t/\Delta x < 1$ . We use  $f$  and  $f'$ ( $\equiv \partial f/\partial x$ ), which is the spatial derivative of  $f$ , as variables in the same way as the CIP method. Furthermore, we add  $\rho$  defined by Eq.(5) as another variable. The  $i$ th function piece  $F_i(x)$  is determined so as to satisfy the continuity condition

$$\begin{cases} F_i(x_{i-1}) = f(x_{i-1}) \\ F_i(x_i) = f(x_i) \\ \partial F_i(x_{i-1})/\partial x = f'(x_{i-1}) \\ \partial F_i(x_i)/\partial x = f'(x_i) \\ \int_{x_{i-1}}^{x_i} F_i(x) dx = \rho_{i-1/2}. \end{cases} \quad (9)$$

In order to meet the above condition, fourth-order

polynomial can be chosen as an interpolation function  $F_i(x)$ :

$$F_i(x) = a_i(x-x_i)^4 + b_i(x-x_i)^3 + c_i(x-x_i)^2 + f'_i(x-x_i) + f_i, \quad (10)$$

Here, each coefficient is determined from five constraints, and taking into consideration of the sign of the velocity, these are given as follows;

$$a_i^n = -\frac{15}{\Delta x_i^4} (f_{iup} + f_i) + \frac{5}{2\Delta x_i^3} (f'_{iup} - f'_i)$$

$$- \operatorname{sgn}(u_i^n) \frac{30}{\Delta x_i^5} \rho_{i-\operatorname{sgn}(u_i^n)/2},$$

$$b_i^n = \frac{4}{\Delta x_i^3} (7f_{iup} + 8f_i) - \frac{4}{\Delta x_i^2} (f'_{iup} - (3/2)f'_i)$$

$$+ \operatorname{sgn}(u_i^n) \frac{60}{\Delta x_i^4} \rho_{i-\operatorname{sgn}(u_i^n)/2},$$

$$c_i^n = -\frac{6}{\Delta x_i^2} (2f_{iup} + 3f_i) + \frac{3}{2\Delta x_i} (f'_{iup} - 3f'_i)$$

$$- \operatorname{sgn}(u_i^n) \frac{30}{\Delta x_i^3} \rho_{i-\operatorname{sgn}(u_i^n)/2},$$

$$\Delta x_i = x_{iup} - x_i,$$

(11)

$$i_{up} = \begin{cases} i-1 & \text{if } u_i^n \geq 0, \\ i+1 & \text{if } u_i^n < 0, \end{cases} \quad \operatorname{sgn}(u_i^n) = \begin{cases} +1 & \text{if } u_i^n \geq 0, \\ -1 & \text{if } u_i^n < 0. \end{cases}$$

For constant velocity field, the spatial derivative of Eq.(7) is given by

$$\frac{\partial f'}{\partial t} + u \frac{\partial f'}{\partial x} = 0, \quad (12)$$

which simply represents the advection of  $f'$  with the same velocity as  $f$  in Eq.(7). Therefore, the time development of  $f$  and  $f'$  is calculated simply by shifting the interpolation function  $F_i(x)$  by  $u\Delta t$  in the same way as the CIP method as follows;

$$f_i^* = F_i(x_i - u_i^n \Delta t) = a_i^n \xi_i^4 + b_i^n \xi_i^3 + c_i^n \xi_i^2 + f_i'^n \xi_i + f_i^n, \quad (13)$$

$$f_i'^* = \partial F_i(x_i - u_i^n \Delta t)/\partial x = 4a_i^n \xi_i^3 + 3b_i^n \xi_i^2 + 2c_i^n \xi_i + f_i'^n, \quad (14)$$

where  $\xi_i = -u_i^n \Delta t$ , and each coefficient is equivalent to Eq.(11) at the time step  $n$ . The problem left for us is to calculate the time development of  $\rho$ . Although there exists a variety of possibilities, the simplest one is to calculate the time development of  $\rho$  based on Eq.(1) to satisfy Eq.(6).  $\rho_{i-1/2}^n$  is equivalent to the sum of  $f$

contained in a cell between grids  $[x_{i-1}, x_i]$ . Therefore, if we define the flux passing through  $x_{i-1}$  and  $x_i$  during  $[t, t+\Delta t]$  as  $\Delta\rho_{i-1}$  and  $\Delta\rho_i$  respectively, the time development of  $\rho$  is calculated by the following equation;

$$\rho_{i-1/2}^{n+1} = \rho_{i-1/2}^n + \Delta\rho_{i-1}^n - \Delta\rho_i^n. \quad (15)$$

With the aid of Fig.1, it is clear that  $\Delta\rho_i^n$  is defined by the following equation;

$$\begin{aligned} \Delta\rho_i^n &= \int_{x_i - u_i^n \Delta t}^{x_i} F_i^n(x) dx \\ &= - \left( \frac{a_i^n}{5} \xi_i^4 + \frac{b_i^n}{4} \xi_i^3 + \frac{c_i^n}{3} \xi_i^2 + \frac{f_i^n}{2} \xi_i + f_i^n \right) \xi_i. \end{aligned} \quad (16)$$

where  $\xi_i = -u_i^n \Delta t$ , and each coefficient is equivalent to Eq.(11) at the time step  $n$ .

Therefore, the solution of Eq.(7) is given by Eqs.(13)~(16). Concerning the initial condition of  $f'$ , we can adopt the following method, for example, in the same way as the CIP method;

$$f_i^0 = \frac{f_{i+1}^0 - f_{i-1}^0}{x_{i+1} - x_{i-1}}. \quad (17)$$

For the initial condition of  $\rho$ , we may interpolate grid interval  $[x_{i-1}, x_i]$  with a straight line. Therefore, the initial condition of  $\rho$  is defined by

$$\rho_{i-1/2}^0 = \frac{f_{i-1}^0 + f_i^0}{2} (x_i - x_{i-1}). \quad (18)$$

### 3. Generalized One-Dimensional Scheme

Next, we discuss the generalized case in which velocity  $u$  can change in space and time. In this case, a conservation law Eq.(1) is put into a form;

$$\frac{\partial f}{\partial t} + u \frac{\partial f}{\partial x} = -f \frac{\partial u}{\partial x}. \quad (19)$$

In order to calculate Eq.(19), we split it into two phases in the same way as the CIP method. One is advection phase;

$$\frac{\partial f}{\partial t} + u \frac{\partial f}{\partial x} = 0, \quad (20)$$

and the other is non-advection phase;

$$\frac{\partial f}{\partial t} = -f \frac{\partial u}{\partial x} \equiv G. \quad (21)$$

The spatial derivative of Eq.(19) can also be split into two phases in the same way as the above argument. Therefore the advection phase is

$$\frac{\partial f'}{\partial t} + u \frac{\partial f'}{\partial x} = 0, \quad (22)$$

and the non-advection phase is

$$\frac{\partial f'}{\partial t} = G' - f' \frac{\partial u}{\partial x}. \quad (23)$$

If we can assume that the velocity  $u$  remains

constant during time interval  $\Delta t$ , we can use the same procedure as Eqs.(13) and (14) for the advection phase.

Therefore Eq.(20) that corresponds to the advection phase of  $f$  is calculated by Eq.(13), and Eq.(22) that is for the advection phase of  $f'$  is calculated by Eq.(14). After  $f$  and  $f'$  are advanced in the advection phase, Eqs.(21),(23) that correspond to the non-advection phase are calculated with a finite-difference approach in the same way as the CIP method. These two phases together with the development of  $\rho$  over one time step given by Eq.(15) complete one time step of the calculation.

It is important to note that the mass conservation is recovered in a form of spatial profile within a grid cell every time step when the polynomial is constructed under the constraint of Eq.(9), even if the separate treatment of Eq.(19) may not guarantee the mass conservation in the sense of Eq.(3).

### 4. Numerical Tests

In this section, we shall present some sample calculations to test the procedure given by Eqs.(13)~(15).

#### I. One-dimensional linear advection problem ( $u = \text{const.}$ )

Let us start at first with linear advection of a square wave under a constant velocity field like  $u=1$  in Eq.(1), and the following initial condition is chosen.

$$f(0, x) = \begin{cases} 1 & \text{if } 40 \leq x \leq 60 \\ 0 & \text{otherwise,} \end{cases}$$

where equally spaced grids points of  $\Delta x=1$  and CFL number of 0.1 are used.

Figure 2 shows the profile after 1000 time steps. For comparison, we also include the result of the CIP method in Fig.3 and the first order upwind scheme in Fig.4 with the same condition. The solid line shows the initial condition that corresponds to the exact solution.

Since we use the interpolation function of the fourth order in Eq.(13), more accurate representation of discontinuity is made possible than the CIP method which uses the interpolation function of the third order. The over and under shoots observed in Fig.2 never grow as well as the CIP method.

## II . Generalized one-dimensional problem ( $u \neq \text{const.}$ )

Next, we slightly modify the above example into variable velocity field and then Eq.(1) is solved under a given velocity field;

$$u = 1 + 0.5 \sin(2\pi x / 100),$$

with the following initial condition,

$$f(0, x) = \begin{cases} 1 & \text{if } 40 \leq x \leq 60 \\ 0 & \text{otherwise,} \end{cases}$$

where equally spaced grids points of  $\Delta x = 100/(N-1)$  and time step size of  $\Delta t = 10/(N-1)$  are used,  $N$  being the number of grid points. In this case, the procedure given by Eqs.(20)~(23) and (15) is employed.

We repeated the calculation by changing the total grid number to  $N = 101, 301$  and  $1001$  to test grid dependence for the present scheme, the CIP scheme and the upwind scheme in Figs.5,6 and 7, respectively. Furthermore, the result of the first order upwind scheme with  $N = 10001$  is added in Fig.7. All profiles are those after  $10(N-1)$  time steps that corresponds to  $t=100$ . Since no analytical solution is available, the result of the present scheme with  $N = 1001$  is shown by the solid line in Figs.6 and 7.

We confirm that the accuracy has been improved at the discontinuity in this calculation as well. It is important to note that the first order upwind scheme needs 10,001 grid points to obtain the same result as the present scheme or the CIP method of 101 grid points, which already converged to one solution regardless of grid size. Furthermore, it has already been shown that most of the modern schemes like TVD and ENO fail to reproduce the result with 101 grid points[9].

Figure 8 shows the conservation error of  $f$  and  $\rho$  in our scheme, and that of  $f$  in the CIP method in the case of  $N = 101$ . The conservation is not always guaranteed with the CIP method since it is non-conservative scheme, although the error is extremely small. The present scheme, however, guarantees the conservation of spatially integrated mass  $\rho$  as proposed in the previous section. Although the exact definition of mass  $\rho$  is conserved as can be observed from Eq.(15),  $\sum f$  is not always kept constant. This discrepancy appears at the beginning of the calculation because the initial profiles are not described by polynomial. After the calculation proceeds, both  $\rho$  and  $\sum f$  give similar results.

## III. Burger's equation without viscosity

The following one-dimensional Burger's equation is an interesting example of application to a non-linear equation;

$$\frac{\partial u}{\partial t} + u \frac{\partial u}{\partial x} = 0. \quad (24)$$

Since Eq.(24) does not have non-advection phase, the time development of  $u$  is calculated only by Eq.(13). In order to calculate spatial derivative of  $u$ , we differentiate Eq.(24), then

$$\frac{\partial u'}{\partial t} + u \frac{\partial u'}{\partial x} = -u'^2.$$

This equation is split into two phases:  $\partial u'/\partial t + u \partial u'/\partial x = 0$  (advection) and  $\partial u'/\partial t = -u'^2$  (non-advection). We calculate the advection phase with Eq.(14), and the non-advection phase with the following equation applying a finite difference method;

$$u_i^{n+1} = u_i^n - (u_i^n)^2 \Delta t.$$

For the calculation of  $\rho (= \int u dx)$ , we transform Eq.(24) into the conservation form as follows;

$$\frac{\partial u}{\partial t} + \frac{\partial (u^2/2)}{\partial x} = 0. \quad (25)$$

From this equation, we update  $\rho$  by the following equation;

$$\begin{aligned} \rho_{i-1/2}^{n+1} &= \rho_{i-1/2}^n + \Delta \rho_i^n - \Delta \rho_{i-1}^n \\ \Delta \rho_i^n &= \int_{x_{i-1/2}}^{x_i} F_i^n(x) dx \\ &= - \left( \frac{a_i^n}{5} \xi_i^4 + \frac{b_i^n}{4} \xi_i^3 + \frac{c_i^n}{3} \xi_i^2 + \frac{f_i^n}{2} \xi_i + f_i^n \right) \xi_i, \end{aligned}$$

where  $\xi_i = -(u/2)_i^n \Delta t$ , and each coefficient is equivalent to Eq.(11).

The initial condition used here is

$$u(0, x) = 0.5 + 0.4 \cos(2\pi x / 100),$$

where equally spaced grid points of  $\Delta x = 100/(N-1)$  and time step size of  $\Delta t = 10/(N-1)$  are used,  $N$  being the number of grid points.

Figure9 shows the calculation result with  $N = 101$  by the present scheme after  $10(N-1)$  time step that corresponds to  $t=100$ . For comparison, we also include the result of the CIP method in Fig.10. In order to check the exact speed of a shock wave, we show the result of the calculation with the conservative form of Burger's equation (Eq.(25)) by the first-order upwind scheme with  $N = 1001$  in Figs.9 and 10.

In this calculation, viscosity term is not considered. Without viscosity term, we can not

correctly calculate the speed of a shock wave by non-conservative scheme like the CIP method in Fig.10, while the speed of a shock wave can be exactly obtained by our scheme as shown in Fig.9.

#### IV. Burger's equation with viscosity

Finally, we solve the Burger's equation with viscosity term as follows;

$$\frac{\partial u}{\partial t} + u \frac{\partial u}{\partial x} = \lambda \frac{\partial^2 u}{\partial x^2}.$$

The viscosity term is calculated with a finite-difference approach. The initial condition is

$$f(0, x) = \begin{cases} 0.9 & \text{if } x \leq 10 \\ -0.1 & \text{if } x > 10, \end{cases}$$

where equally spaced grid points of  $\Delta x = 1.0$  and time step size of  $\Delta t = 0.10$  are used. The coefficient of the viscosity term is set to  $\lambda = 0.15$ .

Figure 11 shows the profile after 1000 time steps that correspond to  $t = 100$  and the propagation speed agrees well with the exact solution.

Although the example given in Fig.9 can be treated by the present scheme without viscosity, the shock wave in Fig.11 dose not propagates without it. This reason is illustrated in Fig.12. When the directions of the flux at the boundaries  $x_1$  and  $x_2$  are opposite, then the total mass at the cell  $B$  should increase. However, as seen from Eqs.(11),(13) and (14),  $f_1$  and  $f_2$  are solely determined from the mass of upwind cells that are  $A$  and  $C$ , respectively. Therefore, the increase of mass at the cell  $B$  is not reflected on the changes of  $f_1$  and  $f_2$ . This is the exceptional case and it happens only when the velocity changes the sign at the neighboring cells and compression occurs.

In the example of Fig.11, the information of mass at the cell  $B$  is redistributed to the neighboring cells through diffusion process. Alternatively, there exists another method to overcome this difficulty. That is to construct a polynomial covering two cells like

$$\begin{aligned} & \tilde{F}_i(x_i - u_i^n \Delta t) \\ & = \tilde{a}_i^n \eta_i^4 + \tilde{b}_i^n \eta_i^3 + \tilde{c}_i^n \eta_i^2 + f_{idw}^{\prime n} \eta_i + f_{idw}^n. \end{aligned} \quad (26)$$

Here,  $i$  corresponds to  $x_1$  for  $u_i > 0$ , and  $idw$  means the downward grid which is  $x_2$  in Fig.12. The polynomial Eq.(26) is defined over the domain  $[x_{up}, x_{idw}] = [x_0, x_2]$ . Supposing the integrated value of  $f$  coincides with  $\rho_A + \rho_B$ , we obtain

$$\begin{aligned} \tilde{a}_i^n &= -\frac{15}{\Delta x_i^4} (f_{up} + f_{idw}) + \frac{5}{2\Delta x_i^3} (f'_{up} - f'_{idw}) \\ & \quad - \text{sgn}(u_i^n) \frac{30}{\Delta x_i^5} (\rho_{i-1/2} + \rho_{i+1/2}), \\ \tilde{b}_i^n &= \frac{4}{\Delta x_i^3} (7f_{up} + 8f_{idw}) - \frac{4}{\Delta x_i^2} (f'_{up} - (3/2)f'_{idw}) \\ & \quad + \text{sgn}(u_i^n) \frac{60}{\Delta x_i^4} (\rho_{i-1/2} + \rho_{i+1/2}), \end{aligned} \quad (27)$$

$$\begin{aligned} \tilde{c}_i^n &= -\frac{6}{\Delta x_i^2} (2f_{up} + 3f_{idw}) + \frac{3}{2\Delta x_i} (f'_{up} - 3f'_{idw}) \\ & \quad - \text{sgn}(u_i^n) \frac{30}{\Delta x_i^3} (\rho_{i-1/2} + \rho_{i+1/2}), \end{aligned}$$

$$\begin{aligned} \Delta x_i &= x_{up} - x_{idw}, \\ iup &= \begin{cases} i-1 & \text{if } u_i^n \geq 0, \\ i+1 & \text{if } u_i^n < 0, \end{cases} \quad idw = \begin{cases} i+1 & \text{if } u_i^n \geq 0, \\ i-1 & \text{if } u_i^n < 0, \end{cases} \\ \text{sgn}(u_i^n) &= \begin{cases} +1 & \text{if } u_i^n \geq 0, \\ -1 & \text{if } u_i^n < 0, \end{cases} \end{aligned}$$

$$\eta_i = x_i - x_{idw} - u_i^n \Delta t.$$

For  $u_i < 0$ ,  $i$  corresponds to  $x_2$ ,  $x_{idw} = x_1$ ,  $x_{up} = x_3$ , and the polynomial is defined over  $[x_{idw}, x_{up}] = [x_1, x_3]$  satisfying the total mass of  $\rho_B + \rho_C$ .

Taking into account of special care using  $\tilde{F}$  at the point shown by Fig.12, the algorithm is slightly changed as

$$\begin{aligned} f_i^* &= \begin{cases} \tilde{F}_i(x_i - u_i^n \Delta t) & \text{if } u_i^n \cdot u_{idw}^n < 0, \\ F_i(x_i - u_i^n \Delta t) & \text{otherwise,} \end{cases} \quad (28) \\ f_i^{\prime*} &= \begin{cases} \partial \tilde{F}_i(x_i - u_i^n \Delta t) / \partial x & \text{if } u_i^n \cdot u_{idw}^n < 0, \\ \partial F_i(x_i - u_i^n \Delta t) / \partial x & \text{otherwise.} \end{cases} \end{aligned}$$

Figure 13 shows the result with  $\lambda = 0$  but Eq.(28) is used. Although a slight undershooting is observed, the propagation speed of the shock wave has been correctly reproduced keeping a quite sharp discontinuity. The use of rational function CIP[10,11] to eliminate the undershooting would be an interesting future problem.

## 5. Conclusion

We have proposed a new algorithm that enables non-conservative schemes to be exactly conservative. In the mass conservation law, mass is used as an additional variable and it corrects the conservation error originated from a non-conservative formulation by continuously changing the shape of interpolation function. By this method, the total mass, which is defined to be

the integrated value of  $f$  over the space, is exactly conserved.

This scheme has been tested by linear advection with variable velocity field and Burger's equation. Although further investigation would improve the result, the present scheme can provide a useful tool to solve nonlinear equation in a non-conservative representation which has been proven to be quite stable for multiphase flow calculations.

The extension of the one-dimensional scheme presented here to multi-dimensions may need a little concern about the introduction of integrated value of  $f$  and will be give in another paper appearing shortly.

### Acknowledgements

This work carried out under the collaborating research program at the National Institute for Fusion Science of Japan. We thank Dr. T. Aoki at the Research Laboratory for Nuclear Reactors in Tokyo Institute of Technology for helpful lecture. We also thank Dr. F. Xiao at Computer Science Laboratory, The Institute of Physical and Chemical Research for careful reading of the manuscript and valuable suggestions.

### References

- [1] H. Takewaki, A. Nishiguchi and T. Yabe : The Cubic-Interpolated Pseudo-Particle (CIP) Method for Solving Hyperbolic-Type Equations *J. Comput. Phys.*, **61** (1985) pp. 261-268.  
 [2] T. Yabe et al. : A Universal Solver for Hyperbolic Equations by Cubic-Polynomial

Interpolation, *Comput. Phys. Commun.* **66** (1991) pp.219-242.

[3] T. Yabe : Unified Solver CIP for Solid, Liquid and Gas, in *CFD Review '98* (World Scientific, 1998).

[4] T. Yabe and F. Xiao : Simulation Technique for Dynamical Evaporation Processes, *Nucl Eng. & Design* **155** (1995) pp.45-53.

[5] S. L. Shapiro and S. A. Teukolsky : Black Holes, White Dwarfs, and Neutron Stars, *John Wiley & Sons, Inc.* (1983).

[6] T. Nakamura and T. Yabe : Cubic Interpolated Propagation Scheme for Solving the Hyper-Dimensional Vlasov-Poisson Equation in Phase Space, *Comput. Phys. Commun.* (1999) in press.

[7] P. K. Smolarkiewicz and J. A. Pudykiewicz : A Class of Semi-Lagrangian Approximations for Fluids, *Journal of the Atmospheric Sciences.* (1992).

[8] A. Staniforth and J. Cote : Semi-Lagrangian Integration Schemes for Atmospheric Models-A Review, *Monthly Weather Review.* (1991).

[9] R. Tanaka, T. Nakamura, T. Yabe and H. Wu : A Class of Conservative Formulation of the CIP Method, *CFD journal* (1999) pp.1-5

[10] F. Xiao, T. Yabe and T. Ito : Constructing Oscillation Preventing Scheme for the Advection Equation by a Rational Function, *Comput. Phys. Commun.* **93** (1996) pp.1-12.

[11] F. Xiao et al. : Constructing a Multi-Dimensional Oscillation Preventing Scheme for the Advection Equation by a Rational Function, *Comput. Phys. Commun.* **94** (1996) pp.103-118.

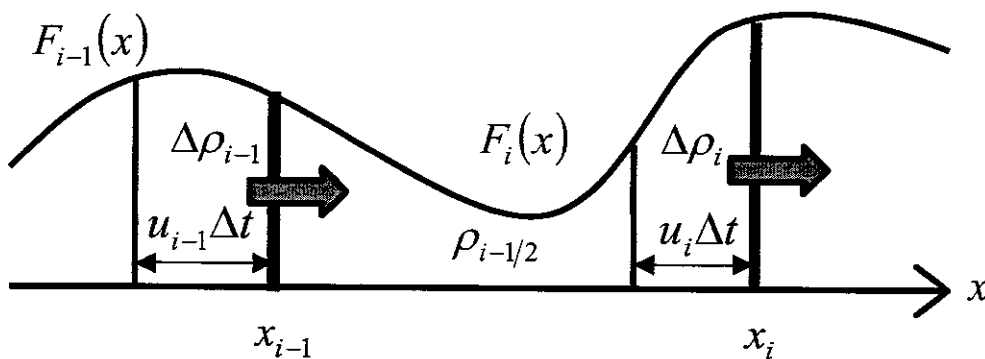


Fig.1 : The inflow and outflow of flux during  $\Delta t$ .

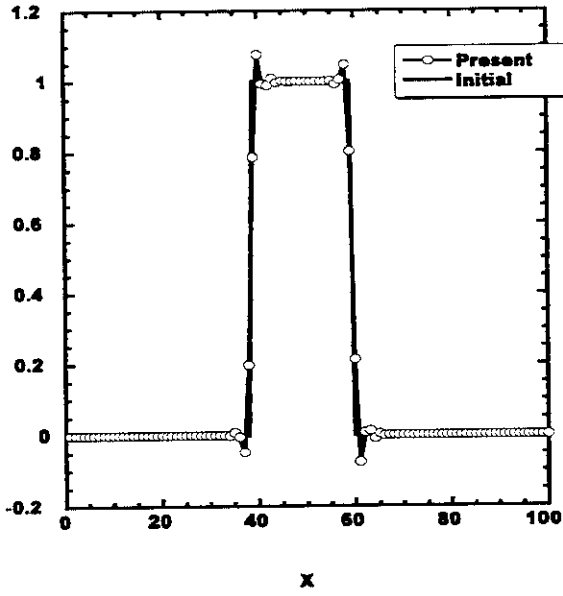


Fig.2: Linear propagation of a square wave after 1000 time steps ( $u\Delta t/\Delta x = 0.1$ ) by the present scheme (circles). The solid line shows the initial profile.

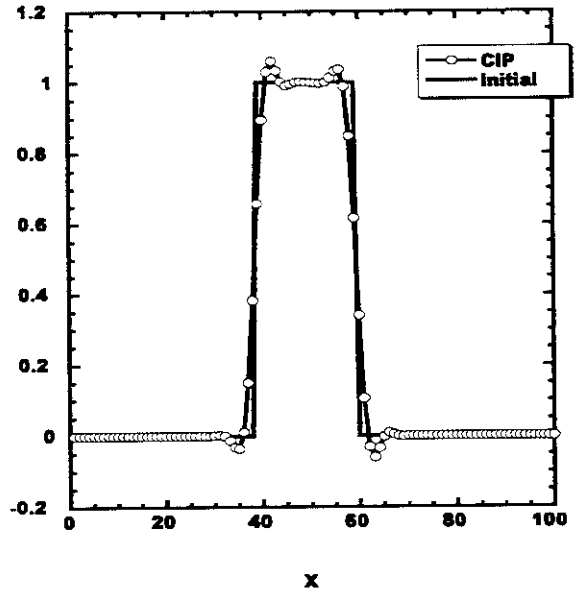


Fig.3: Linear propagation of a square wave after 1000 time steps ( $u\Delta t/\Delta x = 0.1$ ) by the CIP method (circles). The solid line shows the initial profile.

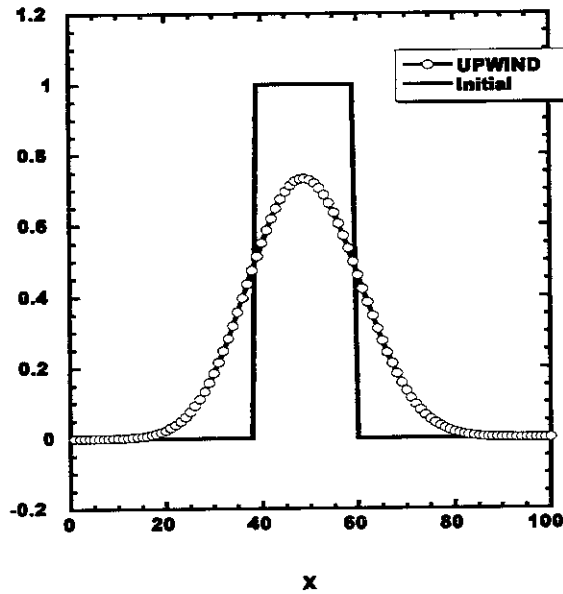


Fig.4: Linear propagation of a square wave after 1000 time steps ( $u\Delta t/\Delta x = 0.1$ ) by the first order upwind (circles). The solid line shows the initial profile.



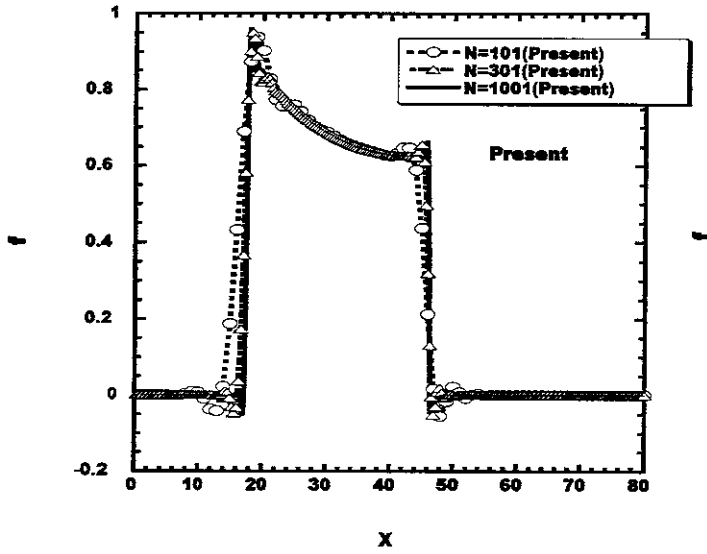


Fig.5: Propagation of a square wave with a given velocity field ( $u=1+0.5\sin(2\pi x/100)$ ) by the present scheme at  $t=100$ . The number of grids is 101(circle), 301(triangle), 1001(solid line).

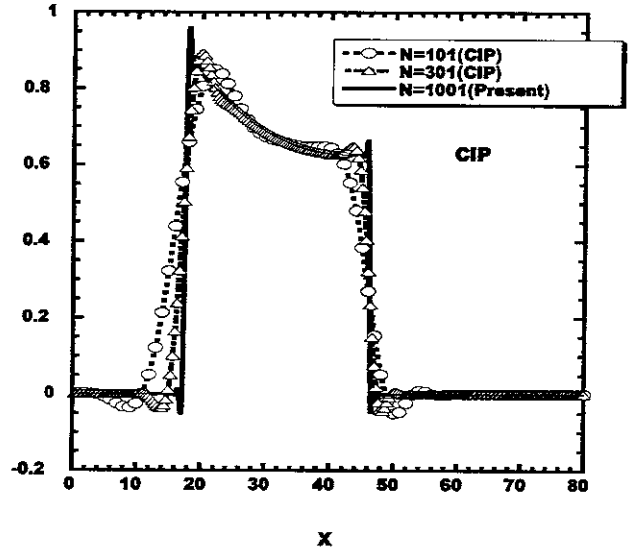


Fig.6: Propagation of a square wave with a given velocity field ( $u=1+0.5\sin(2\pi x/100)$ ) by the CIP method at  $t=100$ . The number of grids is 101(circle), 301(triangle). For comparison, the result of the present scheme of 1001 grids is shown by the solid line.

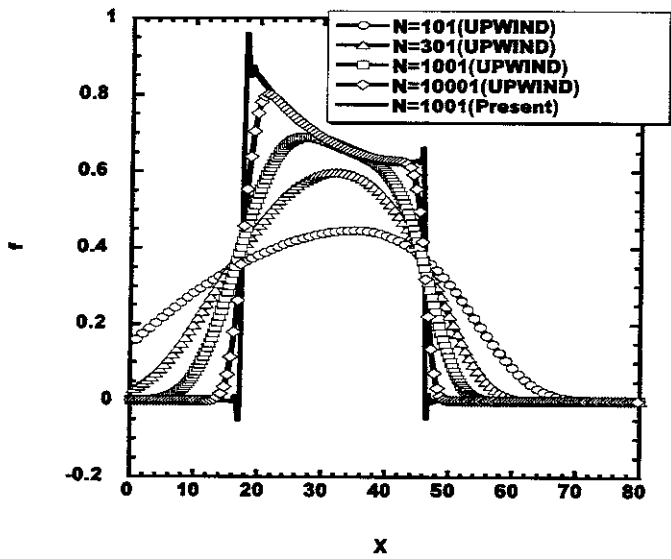


Fig.7: Propagation of a square wave with a given velocity field ( $u=1+0.5\sin(2\pi x/100)$ ) by the first order upwind at  $t=100$ . The number of grids is 101(circle), 301(triangle), 1001(square), 10001(diamond). For comparison, the result of the present scheme of 1001 grids is shown by the solid line.

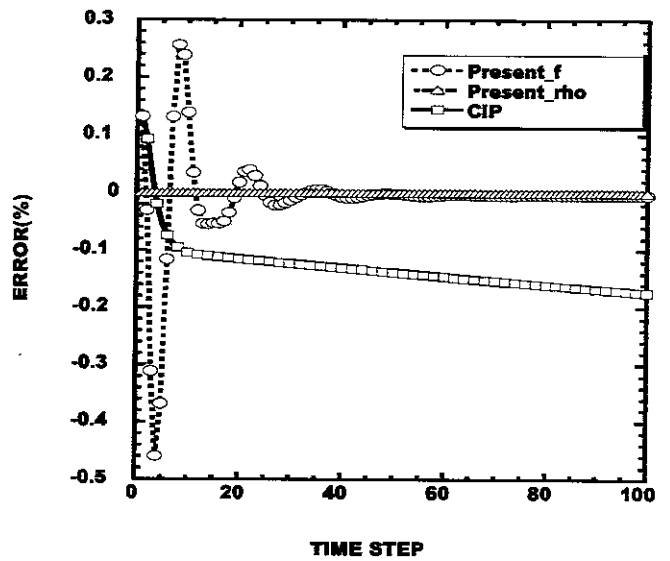


Fig.8 : Conservation error of  $f$  in the present scheme (circle) and the CIP method (square) and  $\rho$  in the present scheme (triangle) until 100 time steps.

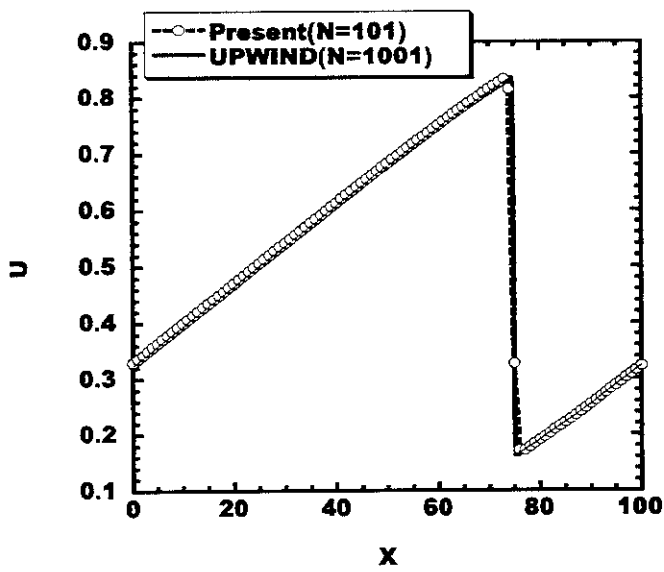


Fig.9: The result of Burger's equation without viscosity by the present scheme with 101 grid points at  $t=100$ . For comparison, the result of the first order upwind scheme with 1001 grid points at  $t=100$  is shown by the solid line.

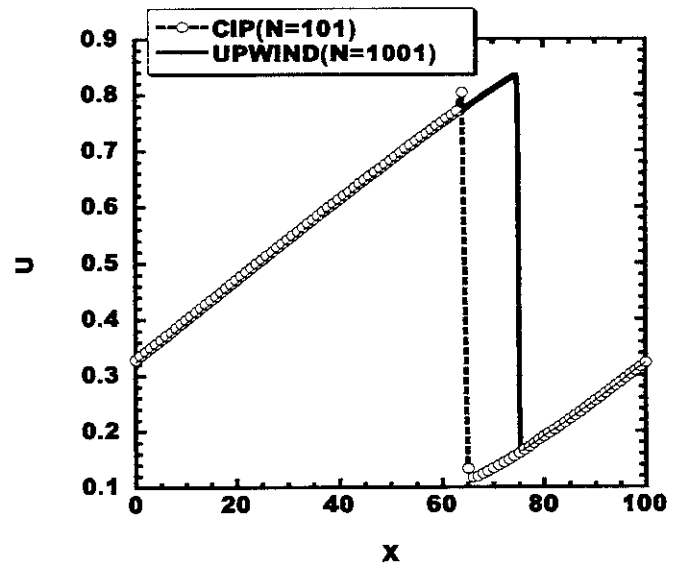


Fig.10: The result of Burger's equation without viscosity by the CIP method with 101 grid points at  $t=100$ . For comparison, the result of the first order upwind scheme with 1001 grid points at  $t=100$  is shown by the solid line.

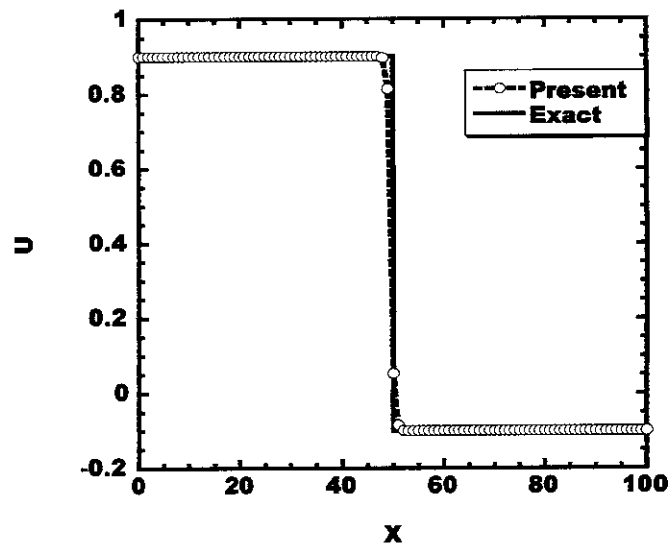


Fig.11: The result of Burger's equation with viscosity by the present scheme at  $t=100$ . The exact solution is shown by the solid line.

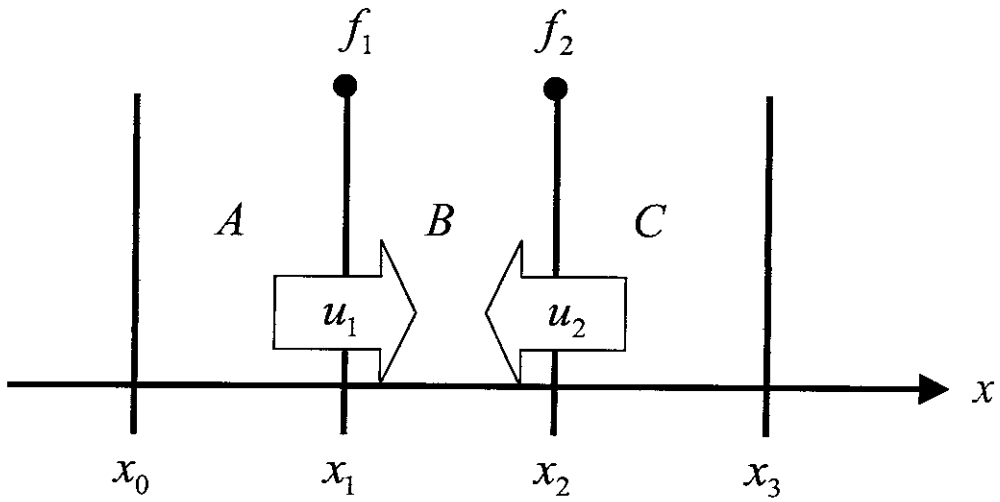


Fig.12: Interpolation for compression phase.

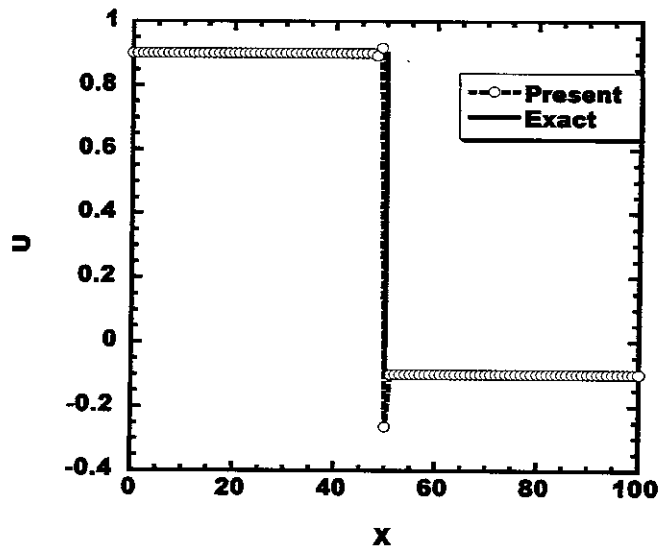


Fig.13: The result of Burger's equation without viscosity by the present scheme at  $t=100$ . The exact solution is shown by the solid line.

## Recent Issues of NIFS Series

- NIFS-545 J Uramoto,  
*Various Neutrino Beams Generated by D<sub>2</sub> Gas Discharge*, Mar 1998
- NIFS-546 R. Kanno, N. Nakajima, T. Hayashi and M. Okamoto,  
*Computational Study of Three Dimensional Equilibria with the Bootstrap Current*, Mar. 1998
- NIFS-547 R. Kanno, N. Nakajima and M. Okamoto,  
*Electron Heat Transport in a Self-Similar Structure of Magnetic Islands*; Apr 1998
- NIFS-548 J.E. Rice,  
*Simulated Impurity Transport in LHD from MIST*; May 1998
- NIFS-549 M.M. Skoric, T. Sato, A.M. Maluckov and M.S. Jovanovic,  
*On Kinetic Complexity in a Three-Wave Interaction*; June 1998
- NIFS-550 S. Goto and S. Kida,  
*Passive Saclar Spectrum in Isotropic Turbulence: Prediction by the Lagrangian Direct-interaction Approximation*; June 1998
- NIFS-551 T. Kuroda, H. Sugama, R. Kanno, M. Okamoto and W. Horton,  
*Initial Value Problem of the Toroidal Ion Temperature Gradient Mode* ; June 1998
- NIFS-552 T. Mutoh, R. Kumazawa, T. Seki, F. Simpo, G. Nomura, T. Ido and T. Watan,  
*Steady State Tests of High Voltage Ceramic Feedthroughs and Co-Axial Transmission Line of ICRF Heating System for the Large Helical Device* ; June 1998
- NIFS-553 N. Noda, K. Tsuzuki, A. Sagara, N. Inoue, T. Muroga,  
*oronaization in Future Devices -Protecting Layer against Tritium and Energetic Neutrals-*: July 1998
- NIFS-554 S. Murakami and H. Saleem,  
*Electromagnetic Effects on Rippling Instability and Tokamak Edge Fluctuations*; July 1998
- NIFS-555 H. Nakamura, K. Ikeda and S. Yamaguchi,  
*Physical Model of Nernst Element*; Aug 1998
- NIFS-556 H. Okumura, S. Yamaguchi, H. Nakamura, K. Ikeda and K. Sawada,  
*Numerical Computation of Thermoelectric and Thermomagnetic Effects*; Aug. 1998
- NIFS-557 Y. Takeiri, M. Osakabe, K. Tsumori, Y. Oka, O. Kaneko, E. Asano, T. Kawamoto, R. Akiyama and M. Tanaka,  
*Development of a High-Current Hydrogen-Negative Ion Source for LHD-NBI System*; Aug.1998
- NIFS-558 M. Tanaka, A. Yu Grosberg and T. Tanaka,  
*Molecular Dynamics of Structure Organization of Polyampholytes*; Sep. 1998
- NIFS-559 R. Horiuchi, K. Nishimura and T. Watanabe,  
*Kinetic Stabilization of Tilt Disruption in Field-Reversed Configurations*; Sep. 1998  
(IAEA-CN-69/THP1/11)
- NIFS-560 S. Sudo, K. Kholopenkov, K. Matsuoka, S. Okamura, C. Takahashi, R. Akiyama, A. Fujisawa, K. Ida, H. Idei, H. Iguchi, M. Isobe, S. Kado, K. Kondo, S. Kubo, H. Kuramoto, T. Minami, S. Monta, S. Nishimura, M. Osakabe, M. Sasao, B. Peterson, K. Tanaka, K. Toi and Y. Yoshimura,  
*Particle Transport Study with Tracer-Encapsulated Solid Pellet Injection*; Oct. 1998  
(IAEA-CN-69/EXP1/18)
- NIFS-561 A. Fujisawa, H. Iguchi, S. Lee, K. Tanaka, T. Minami, Y. Yoshimura, M. Osakabe, K. Matsuoka, S. Okamura, H. Idei, S. Kubo, S. Ohdachi, S. Morita, R. Akiyama, K. Toi, H. Sanuki, K. Itoh, K. Ida, A. Shimizu, S. Takagi, C. Takahashi, M. Kojima, S. Hidekuma, S. Nishimura, M. Isobe, A. Ejiri, N. Inoue, R. Sakamoto, Y. Hamada and M. Fujiwara,  
*Dynamic Behavior Associated with Electric Field Transitions in CHS Heliotron/Torsatron*; Oct 1998  
(IAEA-CN-69/EX5/1)
- NIFS-562 S. Yoshikawa,  
*Next Generation Toroidal Devices*; Oct 1998

- NIFS-563 Y. Todo and T. Sato,  
*Kinetic-Magnetohydrodynamic Simulation Study of Fast Ions and Toroidal Alfvén Eigenmodes*; Oct. 1998  
(IAEA-CN-69/THP2/22)
- NIFS-564 T. Watari, T. Shimozuma, Y. Takeiri, R. Kumazawa, T. Mutoh, M. Sato, O. Kaneko, K. Ohkubo, S. Kubo, H. Idei, Y. Oka, M. Osakabe, T. Seki, K. Tsumori, Y. Yoshimura, R. Akiyama, T. Kawamoto, S. Kobayashi, F. Shimpo, Y. Takita, E. Asano, S. Itoh, G. Nomura, T. Ido, M. Hamabe, M. Fujiwara, A. Iiyoshi, S. Morimoto, T. Bigelow and Y.P. Zhao,  
*Steady State Heating Technology Development for LHD*; Oct. 1998  
(IAEA-CN-69/FTP/21)
- NIFS-565 A. Sagara, K.Y. Watanabe, K. Yamazaki, O. Motojima, M. Fujiwara, O. Mitarai, S. Imagawa, H. Yamanishi, H. Chikaraishi, A. Kohyama, H. Matsui, T. Muroga, T. Noda, N. Ohyabu, T. Satow, A.A. Shishkin, S. Tanaka, T. Terai and T. Uda,  
*LHD-Type Compact Helical Reactors*; Oct. 1998  
(IAEA-CN-69/FTP/03(R))
- NIFS-566 N. Nakajima, J. Chen, K. Ichiguchi and M. Okamoto,  
*Global Mode Analysis of Ideal MHD Modes in L=2 Heliotron/Torsatron Systems*; Oct. 1998  
(IAEA-CN-69/THP1/08)
- NIFS-567 K. Ida, M. Osakabe, K. Tanaka, T. Minami, S. Nishimura, S. Okamura, A. Fujisawa, Y. Yoshimura, S. Kubo, R. Akiyama, D.S. Darrow, H. Idei, H. Iguchi, M. Isobe, S. Kado, T. Kondo, S. Lee, K. Matsuoka, S. Morita, I. Nomura, S. Ohdachi, M. Sasao, A. Shimizu, K. Tsumori, S. Takayama, M. Takechi, S. Takagi, C. Takahashi, K. Toi and T. Watari,  
*Transition from L Mode to High Ion Temperature Mode in CHS Heliotron/Torsatron Plasmas*; Oct. 1998  
(IAEA-CN-69/EX2/2)
- NIFS-568 S. Okamura, K. Matsuoka, R. Akiyama, D.S. Darrow, A. Ejiri, A. Fujisawa, M. Fujiwara, M. Goto, K. Ida, H. Idei, H. Iguchi, N. Inoue, M. Isobe, K. Itoh, S. Kado, K. Khlopenkov, T. Kondo, S. Kubo, A. Lazaros, S. Lee, G. Matsunaga, T. Minami, S. Morita, S. Murakami, N. Nakajima, N. Nikai, S. Nishimura, I. Nomura, S. Ohdachi, K. Ohkuni, M. Osakabe, R. Pavlichenko, B. Peterson, R. Sakamoto, H. Sanuki, M. Sasao, A. Shimizu, Y. Shirai, S. Sudo, S. Takagi, C. Takahashi, S. Takayama, M. Takechi, K. Tanaka, K. Toi, K. Yamazaki, Y. Yoshimura and T. Watari,  
*Confinement Physics Study in a Small Low-Aspect-Ratio Helical Device CHS*; Oct. 1998  
(IAEA-CN-69/OV4/5)
- NIFS-569 M.M. Skoric, T. Sato, A. Maluckov, M.S. Jovanovic,  
*Micro- and Macro-scale Self-organization in a Dissipative Plasma*; Oct. 1998
- NIFS-570 T. Hayashi, N. Mizuguchi, T.H. Watanabe, T. Sato and the Complexity Simulation Group,  
*Nonlinear Simulations of Internal Reconnection Event in Spherical Tokamak*; Oct. 1998  
(IAEA-CN-69/TH3/3)
- NIFS-571 A. Iiyoshi, A. Komori, A. Ejiri, M. Emoto, H. Funaba, M. Goto, K. Ida, H. Idei, S. Inagaki, S. Kado, O. Kaneko, K. Kawahata, S. Kubo, R. Kumazawa, S. Masuzaki, T. Minami, J. Miyazawa, T. Morisaki, S. Morita, S. Murakami, S. Muto, T. Muto, Y. Nagayama, Y. Nakamura, H. Nakanishi, K. Narihara, K. Nishimura, N. Noda, T. Kobuchi, S. Ohdachi, N. Ohyabu, Y. Oka, M. Osakabe, T. Ozaki, B.J. Peterson, A. Sagara, S. Sakakibara, R. Sakamoto, H. Sasao, M. Sasao, K. Sato, M. Sato, T. Seki, T. Shimozuma, M. Shoji, H. Suzuki, Y. Takeiri, K. Tanaka, K. Toi, T. Tokuzawa, K. Tsumori, I. Yamada, H. Yamada, S. Yamaguchi, M. Yokoyama, K.Y. Watanabe, T. Watari, R. Akiyama, H. Chikaraishi, K. Haba, S. Hamaguchi, S. Iima, S. Imagawa, N. Inoue, K. Iwamoto, S. Kitagawa, Y. Kubota, J. Kodaira, R. Maekawa, T. Mito, T. Nagasaka, A. Nishimura, Y. Takita, C. Takahashi, K. Takahata, K. Yamauchi, H. Tamura, T. Tsuzuki, S. Yamada, N. Yanagi, H. Yonezu, Y. Hamada, K. Matsuoka, K. Murai, K. Ohkubo, I. Ohtake, M. Okamoto, S. Sato, T. Satow, S. Sudo, S. Tanahashi, K. Yamazaki, M. Fujiwara and O. Motojima,  
*An Overview of the Large Helical Device Project*; Oct. 1998  
(IAEA-CN-69/OV1/4)
- NIFS-572 M. Fujiwara, H. Yamada, A. Ejiri, M. Emoto, H. Funaba, M. Goto, K. Ida, H. Idei, S. Inagaki, S. Kado, O. Kaneko, K. Kawahata, A. Komori, S. Kubo, R. Kumazawa, S. Masuzaki, T. Minami, J. Miyazawa, T. Morisaki, S. Morita, S. Murakami, S. Muto, T. Muto, Y. Nagayama, Y. Nakamura, H. Nakanishi, K. Narihara, K. Nishimura, N. Noda, T. Kobuchi, S. Ohdachi, N. Ohyabu, Y. Oka, M. Osakabe, T. Ozaki, B. J. Peterson, A. Sagara, S. Sakakibara, R. Sakamoto, H. Sasao, M. Sasao, K. Sato, M. Sato, T. Seki, T. Shimozuma, M. Shoji, H. Suzuki, Y. Takeiri, K. Tanaka, K. Toi, T. Tokuzawa, K. Tsumori, I. Yamada, S. Yamaguchi, M. Yokoyama, K.Y. Watanabe, T. Watari, R. Akiyama, H. Chikaraishi, K. Haba, S. Hamaguchi, M. Iima, S. Imagawa, N. Inoue, K. Iwamoto, S. Kitagawa, Y. Kubota, J. Kodaira, R. Maekawa, T. Mito, T. Nagasaka, A. Nishimura, Y. Takita, C. Takahashi, K. Takahata, K. Yamauchi, H. Tamura, T. Tsuzuki, S. Yamada, N. Yanagi, H. Yonezu, Y. Hamada, K. Matsuoka, K. Murai, K. Ohkubo, I. Ohtake, M. Okamoto, S. Sato, T. Satow, S. Sudo, S. Tanahashi, K. Yamazaki, O. Motojima and A. Iiyoshi,  
*Plasma Confinement Studies in LHD*; Oct. 1998  
(IAEA-CN-69/EX2/3)
- NIFS-573 O. Motojima, K. Akaishi, H. Chikaraishi, H. Funaba, S. Hamaguchi, S. Imagawa, S. Inagaki, N. Inoue, A. Iwamoto, S. Kitagawa, A. Komori, Y. Kubota, R. Maekawa, S. Masuzaki, T. Mito, J. Miyazawa, T. Morisaki, T. Muroga, T. Nagasaka, Y. Nakamura, A. Nishimura, K. Nishimura, N. Noda, N. Ohyabu, S. Sagara, S. Sakakibara, R. Sakamoto, S. Satoh, T. Satow, M. Shoji, H. Suzuki, K. Takahata, H. Tamura, K. Watanabe, H. Yamada, S. Yamada, S. Yamaguchi, K. Yamazaki, N. Yanagi, T. Baba, H. Hayashi, M. Iima, T. Inoue, S. Kato, T. Kato, T. Kondo, S. Morituchi, H. Ogawa, I. Ohtake, K. Ooba, H. Sekiguchi, N. Suzuki, S. Takami, Y. Taniguchi, T. Tsuzuki, N. Yamamoto, K. Yasui, H. Yonezu, M. Fujiwara and A. Iiyoshi,  
*Progress Summary of LHD Engineering Design and Construction*; Oct. 1998  
(IAEA-CN-69/FT2/1)

- NIFS-574 K. Toi, M Takechi, S Takagi, G Matsunaga, M. Isobe, T Kondo, M Sasao, D S Darrow, K Ohkuni, S Ohdachi, R Akiyama, A. Fujisawa, M. Gotoh, H Idei, K. Ida, H Iguchi, S Kado, M Kojima, S. Kubo, S Lee, K. Matsuoka, T. Minami, S. Morita, N. Nikai, S. Nishimura, S. Okamura, M. Osakabe, A. Shimizu, Y. Shirai, C. Takahashi, K. Tanaka, T. Watan and Y. Yoshimura, *Global MHD Modes Excited by Energetic Ions in Heliotron/Torsatron Plasmas*; Oct 1998 (IAEA-CN-69/EXP1/19)
- NIFS-575 Y. Hamada, A. Nishizawa, Y. Kawasumi, A. Fujisawa, M. Kojima, K. Narihara, K. Ida, A. Ejiri, S. Ohdachi, K. Kawahata, K. Toi, K. Sato, T. Seki, H. Iguchi, K. Adachi, S. Hidekuma, S. Hirokura, K. Iwasaki, T. Ido, R. Kumazawa, H. Kuramoto, T. Minami, I. Nomura, M. Sasao, K.N. Sato, T. Tsuzuki, I. Yamada and T. Watan, *Potential Turbulence in Tokamak Plasmas*, Oct 1998 (IAEA-CN-69/EXP2/14)
- NIFS-576 S. Murakami, U. Gasparino, H. Idei, S. Kubo, H. Maassberg, N. Marushchenko, N. Nakajima, M. Romé and M. Okamoto, *5D Simulation Study of Suprathermal Electron Transport in Non-Axisymmetric Plasmas*; Oct. 1998 (IAEA-CN-69/THP1/01)
- NIFS-577 S. Fujiwara and T. Sato, *Molecular Dynamics Simulation of Structure Formation of Short Chain Molecules*; Nov. 1998
- NIFS-578 T. Yamagishi, *Eigenfunctions for Vlasov Equation in Multi-species Plasmas* Nov 1998
- NIFS-579 M. Tanaka, A. Yu Grosberg and T. Tanaka, *Molecular Dynamics of Strongly-Coupled Multichain Coulomb Polymers in Pure and Salt Aqueous Solutions*; Nov 1998
- NIFS-580 J. Chen, N. Nakajima and M. Okamoto, *Global Mode Analysis of Ideal MHD Modes in a Heliotron/Torsatron System: I. Mercier-unstable Equilibria*; Dec. 1998
- NIFS-581 M. Tanaka, A. Yu Grosberg and T. Tanaka, *Comparison of Multichain Coulomb Polymers in Isolated and Periodic Systems: Molecular Dynamics Study*; Jan. 1999
- NIFS-582 V.S. Chan and S. Murakami, *Self-Consistent Electric Field Effect on Electron Transport of ECH Plasmas*; Feb 1999
- NIFS-583 M. Yokoyama, N. Nakajima, M. Okamoto, Y. Nakamura and M. Wakatani, *Roles of Bumpy Field on Collisionless Particle Confinement in Helical-Axis Heliotrons*; Feb. 1999
- NIFS-584 T.-H. Watanabe, T. Hayashi, T. Sato, M. Yamada and H. Ji, *Modeling of Magnetic Island Formation in Magnetic Reconnection Experiment*, Feb. 1999
- NIFS-585 R. Kumazawa, T. Mutoh, T. Seki, F. Shinpo, G. Nomura, T. Ido, T. Watari, Jean-Mane Noterdaeme and Yangping Zhao, *Liquid Stub Tuner for Ion Cyclotron Heating*; Mar. 1999
- NIFS-586 A. Sagara, M. Ima, S. Inagaki, N. Inoue, H. Suzuki, K. Tsuzuki, S. Masuzaki, J. Miyazawa, S. Morita, Y. Nakamura, N. Noda, B. Peterson, S. Sakakibara, T. Shirozuma, H. Yamada, K. Akaishi, H. Chikaraishi, H. Funaba, O. Kaneko, K. Kawahata, A. Komori, N. Ohyaibu, O. Motojima, LHD Exp. Group 1, LHD Exp. Group 2, *Wall Conditioning at the Starting Phase of LHD*; Mar. 1999
- NIFS-587 T. Nakamura and T. Yabe, *Cubic Interpolated Propagation Scheme for Solving the Hyper-Dimensional Vlasov-Poisson Equation in Phase Space*; Mar 1999
- NIFS-588 W.X. Wang, N. Nakajima, S. Murakami and M. Okamoto, *An Accurate  $\delta f$  Method for Neoclassical Transport Calculation*, Mar. 1999
- NIFS-589 K. Kishida, K. Araki, S. Kishiba and K. Suzuki, *Local or Nonlocal? Orthonormal Divergence-free Wavelet Analysis of Nonlinear Interactions in Turbulence*; Mar. 1999
- NIFS-590 K. Araki, K. Suzuki, K. Kishida and S. Kishiba, *Multiresolution Approximation of the Vector Fields on  $T^3$* , Mar. 1999
- NIFS-591 K. Yamazaki, H. Yamada, K.Y. Watanabe, K. Nishimura, S. Yamaguchi, H. Nakanishi, A. Komori, H. Suzuki, T. Mito, H. Chikaraishi, K. Murai, O. Motojima and the LHD Group,

*Overview of the Large Helical Device (LHD) Control System and Its First Operation*; Apr. 1999

- NIFS-592 T. Takahashi and Y. Nakao,  
*Thermonuclear Reactivity of D-T Fusion Plasma with Spin-Polarized Fuel*; Apr. 1999
- NIFS-593 H. Sugama,  
*Damping of Toroidal Ion Temperature Gradient Modes*; Apr. 1999
- NIFS-594 Xiaodong Li ,  
*Analysis of Crowbar Action of High Voltage DC Power Supply in the LHD ICRF System*; Apr. 1999
- NIFS-595 K. Nishimura, R. Horiuchi and T. Sato,  
*Drift-kink Instability Induced by Beam Ions in Field-reversed Configurations*; Apr. 1999
- NIFS-596 Y. Suzuki, T.-H. Watanabe, T. Sato and T. Hayashi,  
*Three-dimensional Simulation Study of Compact Toroid Plasmoid Injection into Magnetized Plasmas*;  
Apr. 1999
- NIFS-597 H. Sanuki, K. Itoh, M. Yokoyama, A. Fujisawa, K. Ida, S. Toda, S.-I. Itoh, M. Yagi and A. Fukuyama,  
*Possibility of Internal Transport Barrier Formation and Electric Field Bifurcation in LHD Plasma*;  
May 1999
- NIFS-598 S. Nakazawa, N. Nakajima, M. Okamoto and N. Ohyabu,  
*One Dimensional Simulation on Stability of Detached Plasma in a Tokamak Divertor*, June 1999
- NIFS-599 S. Murakami, N. Nakajima, M. Okamoto and J. Nhrenberg,  
*Effect of Energetic Ion Loss on ICRF Heating Efficiency and Energy Confinement Time in Heliotrons*;  
June 1999
- NIFS-600 R. Horiuchi and T. Sato,  
*Three-Dimensional Particle Simulation of Plasma Instabilities and Collisionless Reconnection in a Current Sheet*;; June 1999
- NIFS-601 W. Wang, M. Okamoto, N. Nakajima and S. Murakami,  
*Collisional Transport in a Plasma with Steep Gradients*; June 1999
- NIFS-602 T. Mutoh, R. Kumazawa, T. Saki, K. Saito, F. Simpo, G. Nomura, T. Watari, X. Jikang, G. Cattanei, H. Okada, K. Ohkubo, M. Sato, S. Kubo, T. Shimozuma, H. Idei, Y. Yoshimura, O. Kaneko, Y. Takeiri, M. Osakabe, Y. Oka, K. Tsumori, A. Komori, H. Yamada, K. Watanabe, S. Sakakibara, M. Shoji, R. Sakamoto, S. Inagaki, J. Miyazawa, S. Morita, K. Tanaka, B.J. Peterson, S. Murakami, T. Minami, S. Ohdachi, S. Kado, K. Narihara, H. Sasao, H. Suzuki, K. Kawahata, N. Ohyabu, Y. Nakamura, H. Funaba, S. Masuzaki, S. Muto, K. Sato, T. Morisaki, S. Sudo, Y. Nagayama, T. Watanabe, M. Sasao, K. Ida, N. Noda, K. Yamazaki, K. Akaiishi, A. Sagara, K. Nishimura, T. Ozaki, K. Toi, O. Motojima, M. Fujiwara, A. Iiyoshi and LHD Exp. Group 1 and 2,  
*First ICRF Heating Experiment in the Large Helical Device*; July 1999
- NIFS-603 P.C. de Vries, Y. Nagayama, K. Kawahata, S. Inagaki, H. Sasao and K. Nagasaki,  
*Polarization of Electron Cyclotron Emission Spectra in LHD*; July 1999
- NIFS-604 W. Wang, N. Nakajima, M. Okamoto and S. Murakami ,  
 *$\delta f$  Simulation of Ion Neoclassical Transport*; July 1999
- NIFS-605 T. Hayashi, N. Mizuguchi, T. Sato and the Complexity Simulation Group,  
*Numerical Simulation of Internal Reconnection Event in Spherical Tokamak*; July 1999
- NIFS-606 M. Okamoto, N. Nakajima and W. Wang,  
*On the Two Weighting Scheme for  $\delta f$  Collisional Transport Simulation*; Aug. 1999
- NIFS-607 O. Motojima, A.A. Shishkin, S. Inagaki, K. Y. Watanabe,  
*Possible Control Scenario of Radial Electric Field by Loss-Cone-Particle Injection into Helical Device*; Aug. 1999
- NIFS-608 R. Tanaka, T. Nakamura and T. Yabe,  
*Constructing Exactly Conservative Scheme in Non-conservative Form*; Aug. 1999